

Structural Analysis and Optimization of Electric Bike Front Drive with Bottom Bracket Electric Motor

Elmedin Mesic¹, Adnan Masic¹, Enis Muratovic^{1*},
Muamer Delic¹, Salem Hasanbegovic¹

¹ Faculty of Mechanical Engineering, University of Sarajevo, Vilsonovo setaliste 9, 71000 Sarajevo, Bosnia and Herzegovina,

* Corresponding author's e-mail: muratovic@mef.unsa.ba

ABSTRACT

The main objective of this research was to propose a light and practical design solution for electric bike front drive with bottom bracket electric motor. The initial design needs to be redesigned so it can enable simultaneous use of the electric drive and pedal drive, with integration of the front gear shifter. After gathering the basic information linked to the problem and inspecting the initial design solution, the assets and flaws have been identified. The CAD models of the considered possible solutions were developed into FEM models which were used for structural analysis in CAD/CAE software system CATIA. On the basis of the FEM analysis and additional criteria, the optimal solution was chosen, and structural optimization, based on FEM model, was performed. A prototype was manufactured and a mounting process in a place of the initial design was performed. Afterwards, electric bike with mounted prototype was tested under real conditions.

Keywords: design, BB drive, CAD/CAE software, structural analysis, optimization, prototype.

INTRODUCTION

Product design represents difficult, complex, multidisciplinary and time limited process of solving a certain problem. This process originates as a demand for specific product or as a necessity for solving some problem. After a large number of iterations, the construction process finishes with a presentation of the possible solutions for the specific problem. The design process can result in a new product or a redesign of the existing product, eliminating particular limitations linked with dimensions or performance. Modeling of solid objects in three dimensions (3D) enables easy interpretation of the design. This has vital importance for design process, because an image of a real object is conceived, with the possibility of modifying the object.

Finite element method (FEM) represents a numerical method used for acquiring the relevant

data of a modeled construction (displacements, stresses, vibrations, etc.). Thereby, even in the early phases of design process, possibility of obtaining reliable information about the validity of implied dimensions and correctness of estimated design solutions is enabled [1, 2].

Optimization methods are used for “adjusting” the construction in order to make the best possible or the most effective variant, with predefined parameters that must not cross the permitted limits [3]. The optimization criteria are called the goal function and in most cases of design problems they represent volume, i.e. mass that needs to be minimized [4, 5].

Prototype manufacturing is related to physical and digital representation of a certain design, used for gaining answer to a specific question or testing assumptions. Prototype manufacturing is classified as a phase of a design process, but also as a tool for further product development [6].



Fig. 1. Appearance of the initial design mounted on bike

INITIAL DESIGN, FLAWS AND PROBLEMS

Figure 1 shows the initial kit for a bike. It is a conversion kit that turns a classic bike into electric hybrid. In this way, the bike keeps the primary characteristics and has an additional ability of electric drive [7, 8].

This sort of drive implies setting an electric motor near the main drive of a bike, which represents the so-called bottom bracket drive (BB drive). An electric drive is subsequently mounted on the bottom bracket of the bike frame, in front of the main drive. Power is transferred via chains and standard transmission components [9–12]. The electric motor is coupled with the

planetary transmission. The output of the electric motor amounts to 960 W with maximum torque of 140 Nm, while gear ratio is equivalent to 9.33:1.

Figure 2 shows the basic parts that have direct impact on considered problematic. Pedals are designed for mounting on the one way bearing, which enables free rotation of sprocket for the case of electric motor drive, without rotation of pedals. The sprocket carrier represents a connection of the actuating sprockets into a functional unit and it is used for integration of the one way bearing. During the exploitation of the initial design, variety of defects and problems have been noticed. Greater loads applied on construction lead to significant radial movements and vibrations on front drive, which results in common failures of the one way bearing [13]. The initial design solution has limited functionality reflected in a path of the shifter that does not correspond to the distances of the sprockets. Another flaw is a difficult assembly/disassembly process caused by arrangement of individual elements of the construction. It is practically impossible to disassemble the carrier with actuating chain sprockets and one way bearing, without disassembling the pedals and one way bearing first.

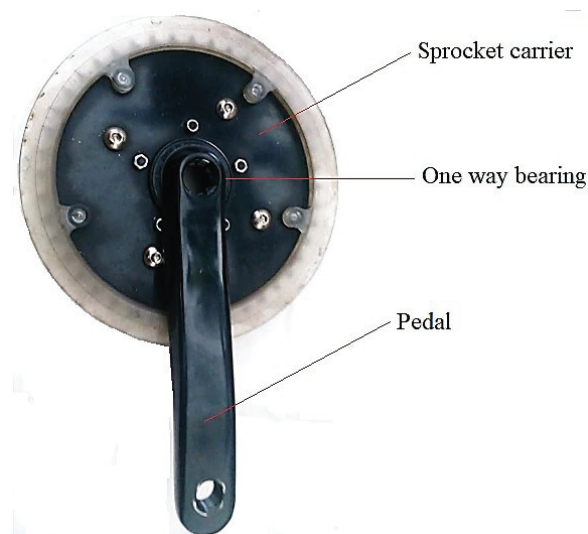


Fig. 2. Basic parts

The above-mentioned flaws and defects serve as a basis for creating a new design solution, i.e. redesigning the initial design solution.

The new solution needs to have a role of a carrier that will enable pedal mounting via one way bearing and actuating sprockets into functional unit. In the continuation of this research

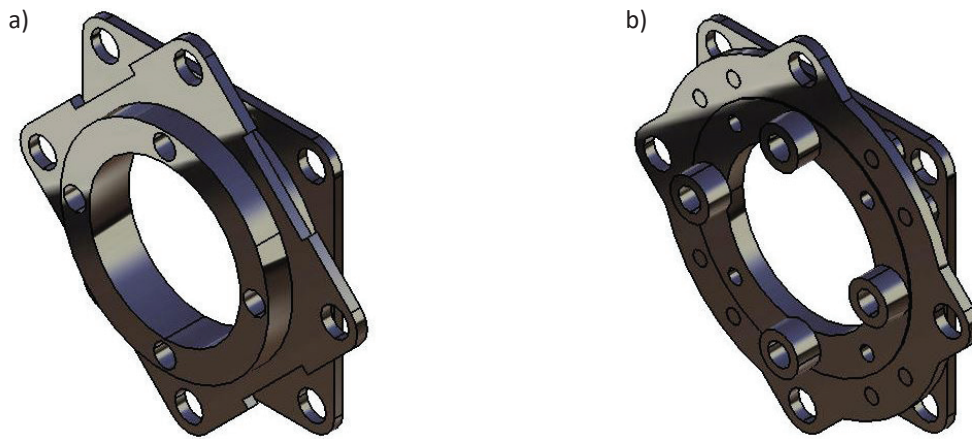


Fig. 3. a) One-piece solution, b) Multi-part solution

this element will be referred as an adapter. The main function of the adapter is power transmission, where power is conducted from two sources, and carried out through one output. This gives three combinations of loads where the most demanding case is the one with both power sources active [14, 15].

CONSIDERED SOLUTIONS

Continuation of this research is considering two solutions. The first solution represents one-part (monolithic) variant, while the other represents a multi-part variant. Generation of these solutions is founded on the variety of factors like: free space, function, integration inside assembly, optimization.

Figure 3a shows the one-part solution of adapter’s design. Unlike the initial design, it is merited with extreme complexity. This solution has smaller stresses in connection elements and in the construction itself. The positive side of a smaller stress condition in connection elements is reflected in decrement of the possible fatigue that can lead to defects.

Figure 3b shows the multi-part adapter. Unlike the initial design, there are no more unappealing and disproportionate flat surfaces. The design is mainly composed from simple components, so that focus is directed to the main part of the carrier whose design satisfies the mass reduction objective.

The main function of the considered solutions is to enable gear ratios changeover. This is accomplished with chain dislocation from one sprocket to the other. Considering this is a front drive, with dislocating chain on a sprocket with less teeth, greater reduction factor is acquired and vice versa. The design contains three sprockets and it demands one reception place for the smallest sprocket and one reception place for medium and large sprocket. Therefore, for every chain position there are suitable working conditions. Further considerations will take into account only the critical conditions for the case of both power sources active. The material chosen for adapter manufacturing is the AlCu6BiPb alloy. This alloy is also known as Free Machining Alloy or “FMA”, which is featured with exceptional machine processing and has wide range of implementation for

Table 1. Mechanical characteristics of the material

Yield strength [MPa]	Fracture strength [MPa]	Shear strength [MPa]	Elongation A5 [%]	Permanent strength [MPa]
270	350	210	18	250

Table 2. Physical characteristics of the material

Melting point [°C]	Density [kg/m³]	Thermal conductivity [W/mK]	Coefficient of thermal expansion [–]	Young’s modulus [GPa]
563	2.82	138	$23 \cdot 10^{-6}$	71

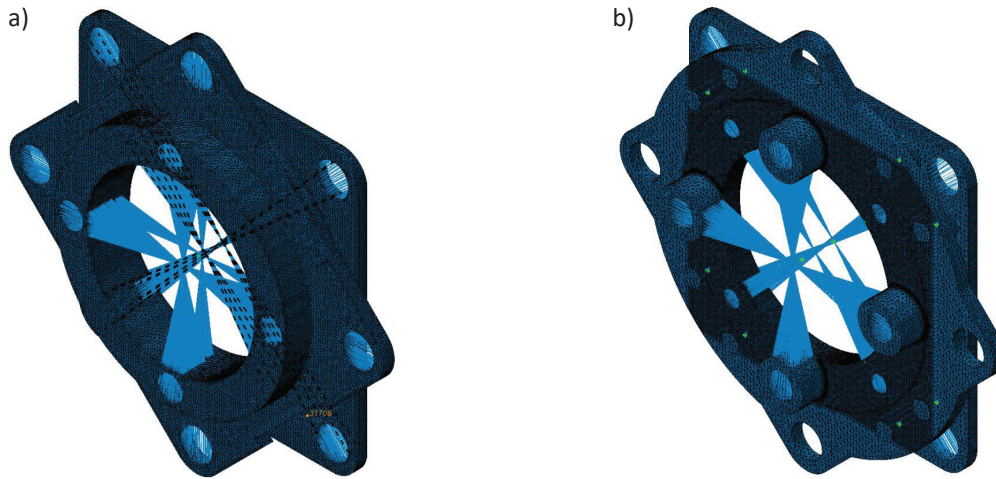


Fig. 4. a) One-piece solution meshing, b) Multi-part solution meshing

parts of extreme complexity. Tables 1 and 2 show the mechanical and physical characteristics of the considered alloy.

FEM ANALYSIS

FEM analysis has been performed in Computer Aided Design/Computer Aided Engineering (CAD/CAE) system CATIA. The analysis process begins with discretization of physical continuum,

i.e. dividing structure on finite elements [16]. The considered variants implemented TE4 elements that have constant strain components (Table 3). The TE4 elements represent linear tetrahedrons which contain 4 nodes in the vertices. Uniform mesh is used for the one-piece solution with the element size of 1 mm and sag of 0.2 mm, which is shown on Fig. 4a. Multi-part solution combined finite elements with the size of 1 mm and sag of 0.2 mm and local mesh with finite elements size of 0.5 mm and sag of 0.1 mm, which is shown in Fig. 4b. Local mesh is necessary because of the multi-part variant complexity. In this way, the FEM model is simplified for further analysis. Local mesh is applied only on the critical zones, so the model overload is avoided and the computation time is shortened.

Table 3. Number of finite elements and nodes for considered solutions

Solution	Number of nodes	Number of finite elements
One-piece	63416	260446
Multi-part	130763	540051

The next step in FEM model development is the setting of loads and constrains. Fig. 5a

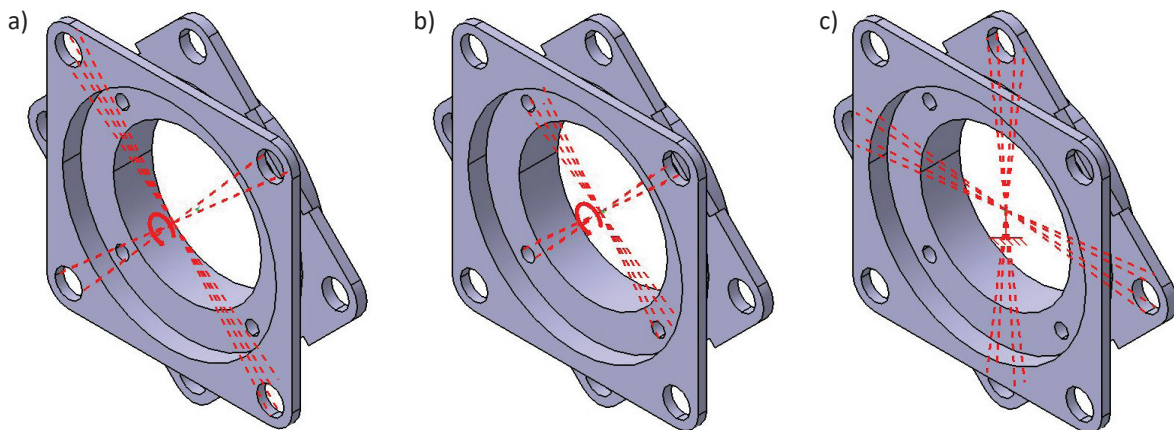


Fig. 5. a) Applying torque from electric motor to one-piece variant, b) Applying torque from pedaling to one-piece variant, c) Applying clamp restraint to one-piece variant

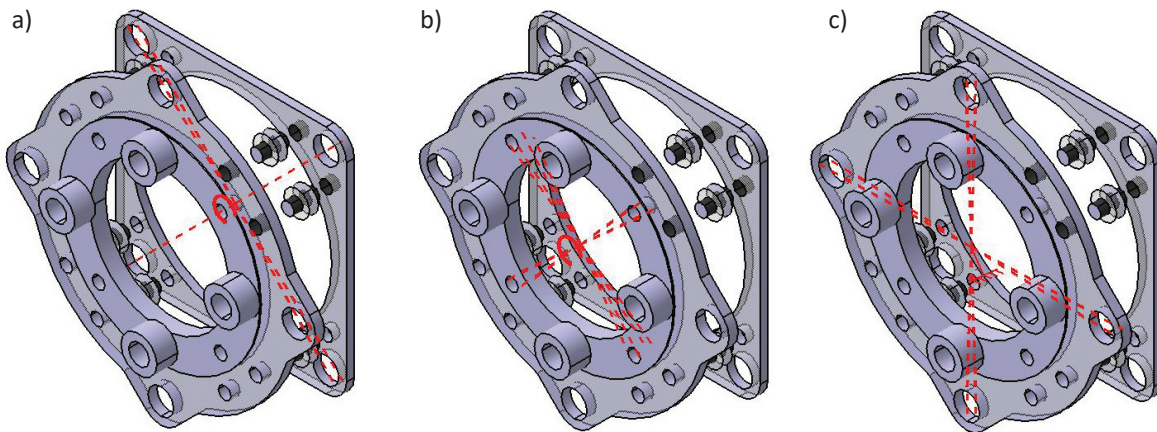


Fig. 6. a) Applying torque from electric motor to multi-part variant, b) Applying torque from pedaling to multi-part variant, c) Applying clamp restraint to multi-part variant

shows the applied load from the electric motor, for the one-piece variant. For the maximum output torque of electric motor equivalent to 140 Nm, load (red curved arrow) is applied on the Virtual Part (red dashed lines) which is connected on the holes designed for mounting of the sprocket actuated by the motor. The function of a Virtual Part is to approximate the impact of the elements that are not modeled. The Virtual Part itself does not have geometry, but it is assumed that elements at the zones of attachment have the same boundary geometry. A similar method is applied for maximum torque obtained by pedaling with the assumed value of 200 Nm. Load is applied on the Virtual Part which is connected with the holes designed for mounting the one-way bearing on the adapter, as shown in Figure 5b. The adapter constrains are approximated with clamp constrain. This

constrain is featured with movement restriction on all degrees of freedom. Clamp is implemented via the Virtual Part which is connected with the assembly holes for the sprocket system, as shown in Figure 5c.

The design contains three sprockets mounted on two places. This results in two cases of analysis. Detailed considerations will be performed for the case which is more demanding for design. The procedure is same for both variants, as shown in Figures 6a, 6b and 6c.

Figure 7a and 7b show Von Mises stresses. This representation gives very clear image in meanings of load transfer through the construction. It is important to remark that both of these solutions, with their characteristics, satisfy the strength criteria.

Figure 7a shows the Von Mises stress of the one-piece solution for the case of the large

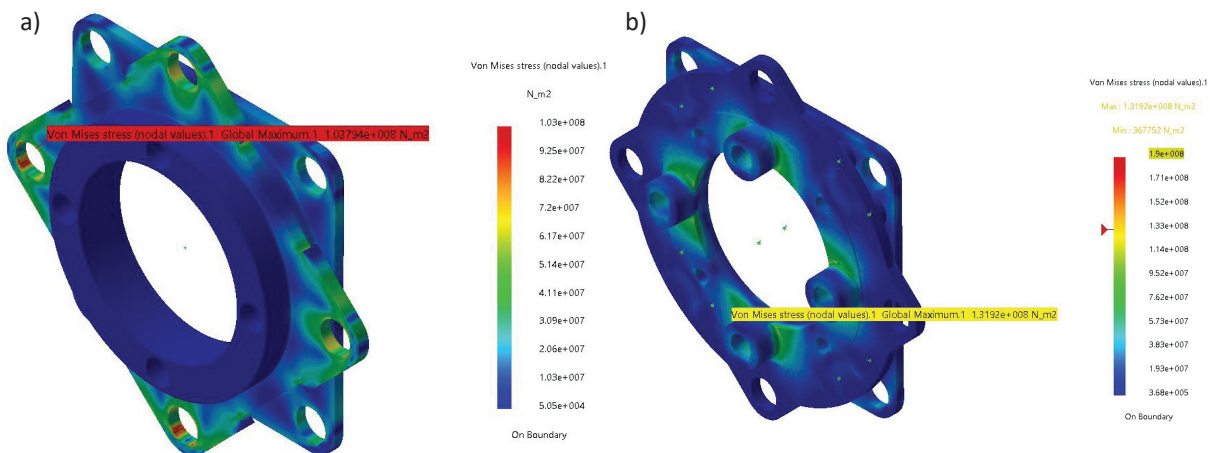


Fig. 7. a) Von Mises stress of the one-piece solution, b) Von Mises stress of the multi-part solution

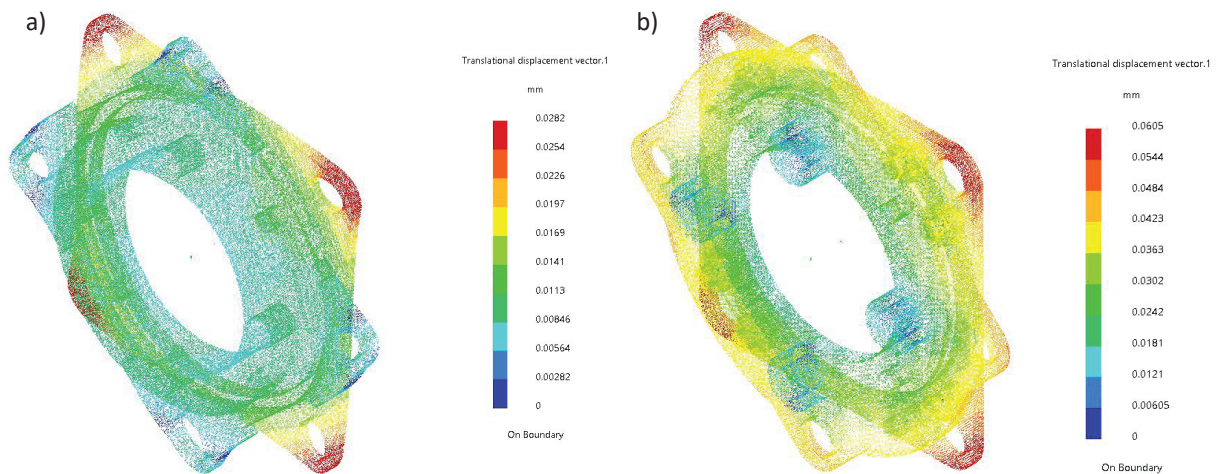


Fig. 8. a) Displacements of the one-piece solution, b) Displacement of the multi-part solution

Table 4. Comparison of one-piece and multi-part analysis results

Parameter	Stress [MPa]	Displacement [mm]
One-piece solution	103	0.0282
Multi-part solution	131.92	0.0605
Difference [%]	24.62%	72.8%

sprocket being actuated, where stress amounts to 103 MPa. Performing stress analysis for the case of small sprocket being actuated results in the stress value of 53.5 MPa. The above-mentioned results imply that variant where load is transferred via the large sprocket is critical, so this variant will be analyzed onwards.

Figure 7b shows the Von Mises stress of the multi-part solution for the case of small sprocket being actuated. Maximum stress amounts to 131.92 MPa. After performing stress analysis for the cases of small and medium sprockets

being actuated, the attained results have smaller values than 131.92 MPa. This indicates that small sprocket actuation will lead to more loaded construction. This condition represents a critical case, so the further considerations will be based on this case. Fig. 8a and Fig. 8b show displacements for both variants.

On the basis of the values of stresses and displacements, according to Table 4, new construction solution is a one-piece variant, primarily because it has more than twice as high stiffness as the multi-part variant.

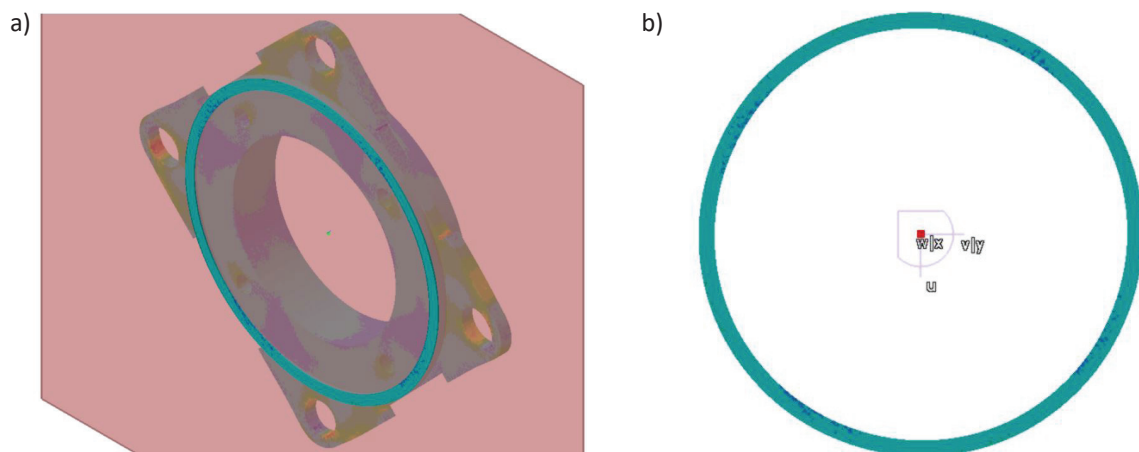


Fig. 9. a) Cross section location, b) Section view

VERIFICATION OF THE FEM ANALYSIS RESULTS

Verification of the FEM analysis results implies comparison of the analysis results with the calculated analytical values (Table 5). Fig. 9a shows the cross section location for the chosen variant between the carrier of sprocket actuated by the electric motor, and the carrier of sprockets actuated with the pedals. The cross section has shape of a circular ring, as shown in Fig. 9b, loaded with torque from electric motor output.

Torque stress is calculated as:

$$\tau = \alpha_k \frac{M_u}{W_0} \tag{1}$$

where: M_u – torque moment (maximum torque from electric motor output), W_0 – polar moment of inertia, α_k – geometrical factor of stress concentration.

Polar moment of inertia for a circular ring is calculated with:

$$W_0 = \frac{r_v^4 - r_u^4}{2r_v} \pi \tag{2}$$

where: r_v – external radius, r_u – internal radius.

Polar moment of inertia is equivalent to:

$$W_0 = \frac{42^4 - 39^4}{2 \cdot 42} \pi = 29854.67 \text{ [mm}^3\text{]} \tag{3}$$

The stress concentration factor is read from the proper diagram, for ratio $\frac{r_v}{r_u} = \frac{42}{39} = 1.07$ and for transition radius of 2 mm, it amounts $\alpha_k = 1.3$ [17, 18]. Maximum shear stresses on the brim of circular ring are equivalent to:

$$\tau = 1.3 \frac{140000}{29854.67} = 6.096 \text{ [MPa]} \tag{4}$$

The maximum shear stresses are calculated via main stresses σ_1 and σ_3 . It is important to consider the main stresses in the nodes of a stress concentration zone [19]. The main stresses in those nodes are directed 45° regarding the cross-section axis, which corresponds to the torque stresses. The values of these stresses are $\sigma_1 = 6.54$ MPa and $\sigma_3 = -5.97$ MPa. Shear torque stress is calculated via:

$$\tau_u = \frac{\sigma_1 - \sigma_3}{2} = \frac{6.54 - (-5.97)}{2} = 6.255 \text{ [MPa]} \tag{5}$$

Table 5. Comparison of analytical results and FEM analysis

Analytic stress result [MPa]	FEM analysis stress result [MPa]	Deviation [%]
6.096	6.255	2.542

OPTIMIZATION

The optimization process is executed in Product Engineering Optimizer module of the CAD/CAE system CATIA. For the considered problematic, Simulated Annealing (SA) method was used. The name of the method is linked with the heating and cooling processes of solid materials, where solid state that forms crystal structure is gained by melting, then slowly cooling, in order to gain as the most correct form of the crystal structure, without any defects. Cooling of the melted material is simulated with the parameter that represents temperature. The parameter is controlled with the Boltzmann’s distribution which implies that system energy E in the case of thermal balance, with temperature T, is distributed according to relation:

$$P(E) = e^{\left(\frac{-E}{kT}\right)} \tag{6}$$

where: $P(E)$ – probability of gaining certain energy level, k – Boltzmann’s constant, T – temperature of thermal balance.

On the basis on the Metropolis criterion, the probability of gaining next state condition depends on the difference between energy levels or objective functions of the two analyzed points (conditions):

$$\Delta E = E_{i+1} - E_i \tag{7}$$

$$\Delta E = \Delta f \tag{8}$$

$$\Delta f = f_{i+1} - f_i \equiv f(x_{i+1}) - f(x_i) \tag{9}$$

The new energy condition or the new possible solution x_{i+1} is defined with the Boltzmann’s distribution:

$$P[E_{i+1}] = \min \begin{cases} e^{\left(\frac{-\Delta E}{kT}\right)}, \Delta E > 0 \\ 1, \Delta E \leq 0 \end{cases} \tag{10}$$

Boltzmann’s constant has a scaling role in the SA method and in most cases it has the value of 1. For $\Delta E \leq 0$ relation (9) gives $P[E_{i+1}] = 1$ where point x_{i+1} is always accepted. This is a logical choice in the context of minimization of the objective function, where value $f_{i+1} = f(x_{i+1})$

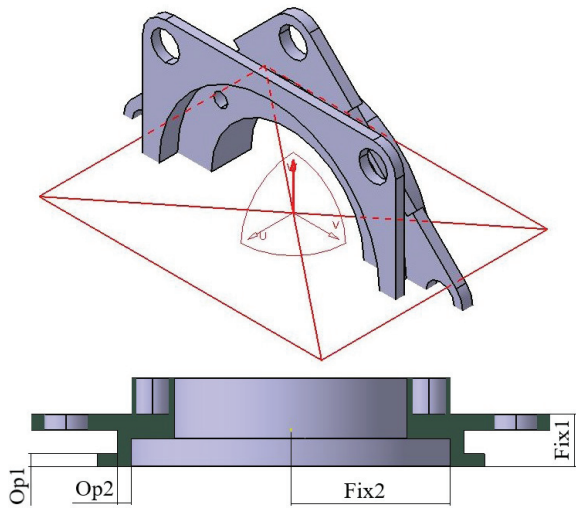


Fig. 10. Design variables for the optimization process

is lower than $f_i = f(x_i)$. Otherwise, when $\Delta E > 0$ value $f_{i+1} = f(x_{i+1})$ is greater than $f_i = f(x_i)$.

It is important to notice that the probability of accepting point x_{i+1} , defined with relation (9), is not equal in all situations and is dependabele of ΔE and T . If temperature T has high value, probability of accepting point x_{i+1} with high values of objective function ΔE will be greater. Therefore, inferior values can be accepted.

This leads to the conclusion that temperature drop (convergence to the optimal solution), decreases the probability of accepting point x_{i+1} with greater values of the objective function regarding to value in point x_i .

The optimization process requires establishment of variables that describe considered

system. These variables are called design variables or design parameters. Different values of these variables lead to a different design solutions. The variables that describe the adapter design are geometric dimensions. It is important that the considered variables are independent of each other and properly selected, so that the final optimization problem could be solved. Fig. 10 shows the optimization variables Op1 and Op2. With a detailed analysis of initial design, it was concluded that two dimensions satisfy the criteria of design variables.

The optimization variable Op1 represents thickness of the adapter zone used for carrying the actuated sprocket. In this case, the optimization problem needs to be configured so that variations of Op1 variable do not have any effect on the dimension Fix1. Fix 1 is a functional dimension which enables necessary distance between the sprockets. The upper limit for Op1 variable amounts to 4 mm, and it is conditioned with working function, where the thickness greater than 4 mm would disable the mounting of a sprocket. The lower limit for Op1 variable amounts to 1 mm and it is conditioned with technologic aspect, where it is not advisable to go under the limit of 1 mm.

The optimization variable Op2 represents the thickness of the transitional adapter zone, which connects the carrier of the actuated sprocket with rest of the construction (Fig. 11). By conducting the FEM analysis, it was established that the stresses in this zone are much lower than the permitted stress value, so this variable is suitable

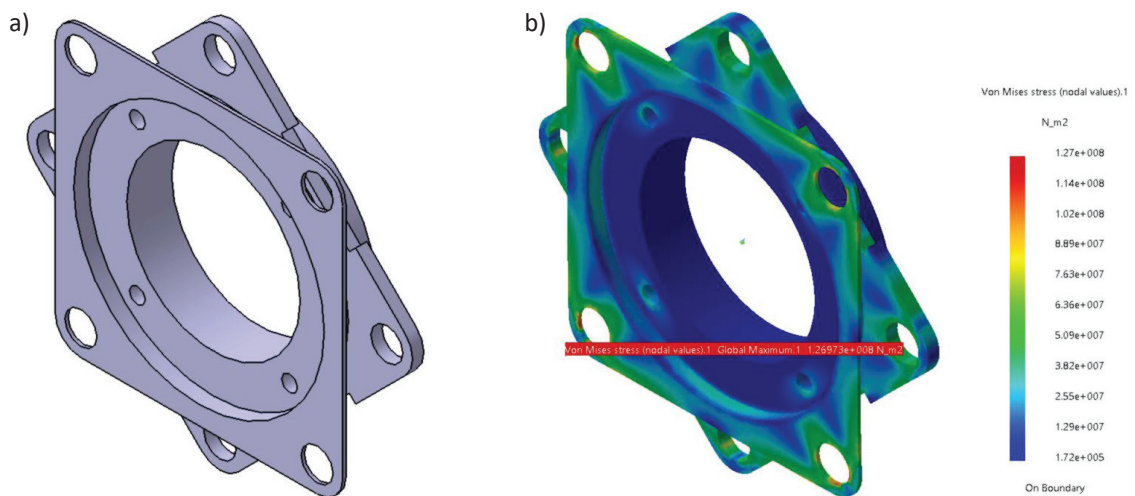


Fig. 11. a) Optimization model, b) Stress results

Table 6. Optimization parameters and limiting values

Parameter	Initial value [mm]	Lower limit [mm]	Upper limit [mm]
Op1	3	1	4
Op2	3	1	5

Table 7. Optimization results

Parameter	Mass [kg]	Stress [MPa]	Displacement [mm]
Initial	0.1323	103	0.302
Optimized	0.1132	127	0.561
Difference	-14.4%	+20%	+85%

for optimization process. Variations of Op2 variable must not affect the radius dimension Fix2. The Fix2 dimension provides centering of the one way bearing in considered assembly. Upper limit for Op2 variable amounts to 5 mm, and it is conditioned with necessary space for sprocket mounting, while lower limit amounts to 1 mm, which corresponds to the manufacturing aspect. Table 6. shows the optimization parameters along with their limiting values.

Optimization is evaluated by the criterion that needs to be scalar dimension. This criterion is called the objective function, which represents mass of the adapter that needs to be minimized [20]. Varying parameters Op1 and Op2 leads to a design with minimum possible mass. Constrains are represented as maximum stresses and maximum displacements. The maximum permitted stress is conditioned by material. The characteristics of

the AlCu6BiPb alloy are shown in Tables 1 and 2. The fracture strength amounts 350 MPa, while the yield strength amounts 270 MPa. For design with dynamic load and minimum mass requirements, safety factor $S = 1.5$ is acquired, which is used to calculate the permitted stress:

$$\sigma_d = \frac{\sigma_v}{S} = \frac{270}{1,5} = 180 \text{ MPa} \quad (11)$$

where: σ_d – permitted stress, σ_v – yield strength, S – safety factor.

The maximum permitted displacement amounts to 1 mm and it is determined from the empirical data, for this type of construction. Optimization results are shown in Table 7 along with the percentage difference between the optimized and initial values. After the optimization process is completed, the design variables Op1 and Op2 gain values of 1 mm, which corresponds to lower variable limits. Although optimization variables reached their boundary values, maximum permitted stress is not exceeded. This leads to the conclusion that optimization variables could reach even smaller values, but manufacturing adapter with those values would be impracticable (Fig. 12). Optimized values satisfy the stress and displacements requirements.

CONCLUSIONS

This paper demonstrated the process of product redesign in accordance with the functionality requirements, production technologies, assembly characteristics, toughness and stiffness. The



Fig. 12. Redesigned adapter mounted on bike

need for redesign emerges in the cases where the initial design falls short of its function by one or many aspects, where exploitation is aggravated directly or indirectly. New design solution needs to resolve the existing flaws, but also set basis for further improvements and considerations. The 3D modeling of construction process was featured with visualization and manipulation of the required objects. This manner enables a simple creation of the design solutions that was used for structural analysis. The FEM analysis represents the first step in creating the optimal solution. The stress and displacement images give information about the construction loads.

The redesign process does not end with the choice of a design solution. Although the design solution satisfies stress and displacement constraints, it is necessary to perform optimization. The optimization process varies set of parameters between determined limits, in order to accomplish the objective function, which, in most cases, is mass minimization. The importance of an optimization process is best reflected in a mass production, where great savings of the material are achieved. The work resulted in manufacturing a prototype that was later on tested under real conditions.

REFERENCES

- Mesic, E., Muminovic, A., Delic, M., Colic, M. and Pervan, N. Topological optimization and finite element method analysis of wheels on the carts winch bridge crane. *TEM Journal*, 8(4), 2019, 1288-1294.
- Uludamar, E., Yıldızhan, Ş., Tosun, E. and Aydın, K. Finite element analysis of electric bike rims coupled with hub motor. *Adv Automob Eng*, 5(2), 2016, 1-4.
- Mesic, E., Muminović, A., Colic, M., Petrovic, M. and Pervan, N. Structural size optimization of external fixation device. *Advances in Science and Technology Research Journal*, 14(2), 2020, 233–240.
- Pervan, N., Muminovic, A.J., Mesic, E., Colic, M. and Hadziabdic, V. Dimensional structural mass optimization of a welded I-profile bridge crane girder. *The. Vjesn.*, 14(2), 2020, 186-193.
- Muminovic, A.J., Muminovic, A., Mesic, E., Saric, I. and Pervan, N. Spur gear tooth topology optimization: finding optimal shell thickness for spur gear tooth produced using additive manufacturing, *TEM Journal*, 8(3), 2019, 788-794.
- Jensen, M.B., Elverum, C.W. and Steinert, M. Eliciting unknown unknowns with prototypes: Introducing prototrials and prototrial-driven cultures. *Design Studies*, 49, 2017, 1–31.
- Machedon-Pisu, M. and Borza, P.N. Are personal electric vehicles sustainable? A Hybrid E-Bike Case Study. *Sustainability*, 12(1), 2020, 1-24.
- Ilahi, T., Zahid, T., Zahid, M., Iqbal, M., Sindhila, A. and Tahir, Q. Design parameter and simulation analysis of electric bike using bi-directional power converter. 2020 International Conference on Electrical, Communication, and Computer Engineering (ICECCE), Istanbul, Turkey, 2020, 1-6.
- Gabor, R., Kowol, M., Kołodziej, J. and Mynarek, P. Steady state analysis of switched reluctance motor with modified geometry of stator designed for an electric bike. 2018 International Symposium on Electrical Machines (SME), Andrychów, 2018, 1-5.
- Tsai, C.Y. A novel design of an electric power assisted bike based on helical gears. *Transactions of the Canadian Society for Mechanical Engineering*, 41(5), 2017, 845-854.
- Sarvesha, Y.V. and Narula, S. Analytical modeling and designing of SMPMSM for electric bike application. 2019 4th International Conference on Electrical, Electronics, Communication, Computer Technologies and Optimization Techniques (ICEECOT), Mysuru, India, 2019, 118-124.
- McLoughlin, I.V., Narendra, I.K., Koh, L.H. Nguyen, Q.H., Seshadri, B., Zeng, W. and Yao, C. Campus mobility for the future: The electric bicycle. *Journal of Transportation Technologies*, 2(1), 2012, 1-12.
- Abagnale, C., Cardone, M., Iodice, P., Strano, S., Terzo, M. and Vorraro, G. Design and development of an innovative e-bike. *Energy Procedia*, 101, 2016, 774-781.
- Matey, S., Prajapati, D.R., Shinde, K., Mhaske, A. and Prabhu, A. Design and fabrication of electric bike. *International Journal of Mechanical Engineering and Technology*, 8(3), 2017, 245–253.
- Raj, A., Paitandi, S. and Sengupta, M. Design validation and performance evaluation of a BLDC of a commercial electric bike and its performance comparison with different probable designs. 2019 National Power Electronics Conference (NPEC), Tiruchirappalli, India, 2019, 1-6.
- Zienkiewicz, O.C. and Taylor, R.L. *The Finite element method – Vol. 2: Solid mechanics*, 5th edition. Butterworth-Heinemann, Oxford, 2003.
- Spotts, M.F., Shoup, T.E. and Hornberger, L.E. *Design of the machine elements*, 8th edition. Prentice Hall, Upper Saddle River, New Jersey, 2004.
- Suchy, I. *Handbook of die design*, 2nd edition. McGraw-Hill, New York, 2006.
- Shigley, J.E., Mischke, C.R. and Budynas, R.G. *Mechanical engineering design*, 7th edition. McGraw-Hill, New York, 2004.
- Muminovic, A.J., Colic, M., Mesic, E. and Saric, I. Innovative design of spur gear tooth with infill structure. *Bull. Pol. Ac.:Tech*, 68(3), 2020, 477-483.